coatings

MDPI

Article

Bodipy-Loaded Micelles Based on Polylactide as Surface Coating for Photodynamic Control of *Staphylococcus aureus*

Enrico Caruso [1], Viviana Teresa Orlandi [1], Miryam Chiara Malacarne [1], Eleonora Martegani [1], Chiara Scanferla [1], Daniela Pappalardo [2], Giovanni Vigliotta [3] and Lorella Izzo [1,*]

[1] Dipartimento di Biotecnologie e Scienze della Vita, Università degli Studi dell'Insubria, 21100 Varese, Italy; enrico.caruso@uninsubria.it (E.C.); viviana.orlandi@uninsubria.it (V.T.O.); mc.malacarne@uninsubria.it (M.C.M.); e.martegani@uninsubria.it (E.M.); cscanferla@uninsubria.it (C.S.)
[2] Dipartimento di Scienze e Tecnologie, Università degli Studi del Sannio, 82100 Benevento, Italy; pappal@unisannio.it
[3] Dipartimento di Chimica e Biologia, Università degli Studi di Salerno, 84084 Fisciano, Italy; gvigliotta@unisa.it
* Correspondence: lorella.izzo@uninsubria.it

Abstract: Decontaminating coating systems (DCSs) represent a challenge against pathogenic bacteria that may colonize hospital surfaces, causing several important infections. In this respect, surface coatings comprising photosensitizers (PSs) are promising but still controversial for several limitations. PSs act through a mechanism of antimicrobial photodynamic inactivation (aPDI) due to formation of reactive oxygen species (ROS) after light irradiation. However, ROS are partially deactivated during their diffusion through a coating matrix; moreover, coatings should allow oxygen penetration that in contact with the activated PS would generate $^1O_2$, an active specie against bacteria. In the attempt to circumvent such constraints, we report a spray DCS made of micelles loaded with a PS belonging to the BODIPY family (2,6-diiodo-1,3,5,7-tetramethyl-8-(2,6-dichlorophenyl)-4,4′-difluoroboradiazaindacene) that is released in a controlled manner and then activated outside the coating. For this aim, we synthesized several amphiphilic copolymers (mPEG–$(PLA)_n$), which form micelles, and established the most stable supramolecular system in terms of critical micelle concentration (CMC) and ΔG_f values. We found that micelles obtained from mPEG–$(PLLA)_2$ were the most thermodynamically stable and able to release BODIPY in a relatively short period of time (about 80% in 6 h). Interestingly, the BODIPY released showed excellent activity against *Staphylococcus aureus* even at micromolar concentrations.

Keywords: polylactide; photodynamic; supramolecular systems; micelles; drug delivery; copolymers; ring opening polymerization; aPDT; BODIPY

Citation: Caruso, E.; Orlandi, V.T.; Malacarne, M.C.; Martegani, E.; Scanferla, C.; Pappalardo, D.; Vigliotta, G.; Izzo, L. Bodipy-Loaded Micelles Based on Polylactide as Surface Coating for Photodynamic Control of *Staphylococcus aureus*. *Coatings* **2021**, *11*, 223. https://doi.org/10.3390/coatings11020223

Academic Editor: Sami Rtimi
Received: 29 December 2020
Accepted: 8 February 2021
Published: 13 February 2021

1. Introduction

One of the route of pathogen dissemination is via contaminated surfaces, as most bacteria can survive for a long time even on the surface of objects. Nosocomial infections generated by contaminated surfaces are a great concern because common disinfectants used in routine cleansing are generally based on quaternary ammonium compounds (QACs), halogen releasing agents, and phenolics, in some cases resulting in ineffective killing of pathogenic bacteria, as their activity depends on several factors, including the surface contact period, pH, temperature, and amount and nature of the microorganism [1].

In the past two decades, to obtain decontamination systems, different antimicrobial substances have been incorporated in the bulk or in the coating of biomaterials. They can be added during the phase of production, a posteriori absorbed in biomaterials, or covalently bound to functionalized polymeric coatings [2].

The storage of anti-pathogens in bulk materials is one of the approaches used for the purpose of gradually releasing biocide, which provides sustained release that kills

pathogens. However, an excessive use of antibiotics leads to the development of antibiotic-resistant pathogens and could causes environmental contamination [3].

Among biocides that can be encapsulated as alternatives to antibiotics, such as phytocomplex, natural, and synthetic peptides [4–6], photosensitizers (PSs) represent a very promising alternative strategy based on the antimicrobial photodynamic inactivation (aPDI) of microorganism. PSs are molecules that, once irradiated with light of a specific wavelength, can reach a relatively long-lived triplet state able to transfer energy to molecular oxygen. The process leads to the formation of the reactive singlet oxygen ($^1O_2$) or, more in general, to reactive oxygen species (ROS) that together induce oxidation reactions resulting in the death of bacteria. Recently, materials containing PSs have been synthesized, characterized, and tested as coatings with antimicrobial efficiency for decontaminating surfaces. Although this strategy allows for the control of multidrug-resistant strains and the inhibition of biofilm formation [7], several requirements limit its application.

To deliver PSs, Hamblin [8] recently proposed some types of nano-drug systems, such as liposomes and micelles. For example, the photoinactivation of *Staphylococcus aureus* by chlorophyll derivatives was increased by the use of liposomes compared to micelles, suggesting that this delivery system is promising in aPDI applications [9]. Furthermore, light-based techniques are believed to be a potent method to counteract microbial biofilms. Thus, the delivery of PSs represents an important goal to reach. To this aim, the PS chlorin e6 (Ce6) was grafted to α-cyclodextrin (α-CD)/polyethylene glycol (PEG). The supramolecular micellar assembly of Ce6 showed enhanced inhibition of biofilm formation of methicillin-resistant *Staphylococcus aureus* (MRSA) [10]. In clinical applications, new delivery systems could overcome undesired damage to normal cells, ascribable to the nonselective nature of photodynamic therapy (PDT). In addition, in decontaminating coating systems based, for example, on polymer matrixes, PSs may be located in polymer layers or polymers fibers. The antimicrobial activity is generated by the PDI process following ROS diffusion through the matrix.

McCoy et al. [11] reported a two-layer system based on PSs incorporated into high density polyethylene (HDPE) through hot-melt extrusion. One layer consisted of a PS contained in HDPE, while the second was made with HDPE alone. Systems containing different PSs were able to reduce the adherence of viable bacteria by up to 3.62 Log colony forming units (CFU) per cm^2 of surface for methicillin-resistant *Staphylococcus aureus* (MRSA) and by up to 1.51 Log CFU/cm^2 for *Escherichia coli*. However, they found that PS chemical compatibility with HDPE was essential to provide complete miscibility of PS with the polymer and consequently homogeneity in PS distribution into the matrix; additionally, with some of the PSs used, the surface of materials showed roughness and irregularity that promoted adhesion of bacteria.

Recently, electrospinning-based technology allowed PS-doped electro-spun materials to be developed, and consequently several systems containing PSs have been proposed as antimicrobial coatings. In this case, photodynamic antimicrobial activity was compromised by the presence of photodynamic molecules into nanofibers, considering that ROS possess short lifetime (less than 3.5 μs) and short diffusion length (about 10–100 nm) [12–17].

In this framework, Felgenträger et al. [18] developed a polymeric surface coating consisting of a derivative of meso-tetraphenyl porphyrin (TPP) immobilized onto polyurethane (PU) after being sprayed and polymerized as a thin layer onto a surface of poly-methylmethacrylate (PMMA). PU is gas permeable and thus was chosen to guarantee that enough oxygen reached the PS into the coating to produce $^1O_2$. Even if the diffusion of ROS was proved by the reduction of bacteria on the surface, the $^1O_2$ luminescence signal exhibited multi-exponential decay, which the authors attributed to a deactivation in the surroundings, such as PU, PMMA, or air.

To overcome limitations of polymer coatings containing PSs, we report here a spray-coating system based on degradable polymer micelles made of poly(ethylene glycol) monomethylether-*co*-polylactide branched copolymers of the general structure mPEG–$(PLA)_n$ (Mn_{mPEG} = 5 kDa, n = 1, 2, or 4), releasing a PS. The same copolymers were previously

obtained in both micro- and nanometric formulations and previously described also as drug delivery systems [19–21]. The photoactive molecule was chosen among the 4,4-difluoro-4-bora-3a,4a-diaza-s-indacene (BODIPY) dyes family, which are characterized to be strongly UV-absorbing and to have high quantum efficiencies of fluorescence. They are also relatively insensitive to the polarity and pH of the environment and are reasonably stable in physiological conditions. BODIPY-based dyes are generally considered an interesting class of compounds for antimicrobial photodynamic therapy (aPDT), as they maintain photochemical properties, even when modified, by introducing substituent groups in some positions of the molecule [22–24]. In the present study, micelle coating surfaces worked as micro-reservoirs of BODIPY, which was released on the surface in a controlled manner.

Overall, surface decontamination with the micelle coating was thought as a process consisting of the release of BODIPY in a relatively short period of time during which the PS is continuously activated by irradiation. The aim is to realize a decontamination treatment through a "spray-coating" capable of removing bacteria completely and deeply from surfaces, avoiding ROS diffusion through the coating matrix and their partial deactivation.

2. Materials and Methods

2.1. Materials

All manipulations involving air-sensitive compounds were carried out under nitrogen atmosphere using Schlenk or dry-box techniques. Poly(ethylene glycol) monomethyl ether (mPEG, M_n = 5000 Da) was purchased from Aldrich and dried in vacuo over phosphorus pentoxide for 72 h at 25 °C prior to use (Aldrich). L- and D,L-lactide, purchased from Aldrich, were crystallized from dry toluene, then dried in vacuo with phosphorus pentoxide for 72 h at 25 °C. Toluene, purchased from Aldrich, was dried over sodium and distilled before use. $Al(CH_3)_3$, phosphorus pentoxide, and pyrene were supplied from Aldrich and used as received. Dichloromethane (DCM) and dimethyl sulfoxide (DMSO) were purchased from Carlo Erba and used without purification. Dialysis was performed with Orange Scientific membrane and OrDial D35-MWCO 3500 regenerated cellulose dialysis tubing. The compound 2,6-diiodo-1,3,5,7-tetramethyl-8-(2,6-dichlorophenyl)-4,4′-difluoroboradiazaindacene was synthetized as previously reported [25].

2.2. Synthesis of mPEG–$(PLA)_n$ Copolymers

The copolymers used in this work were synthesized according to the procedures reported in the literature [19] by using a PEG/LA ratio (*w*/*w*) of 1/2.

A typical procedure is herein described for the copolymer of entry 1 and 2 (Table 1). A magnetically stirred reactor vessel (50 mL) was charged sequentially with a solution of mPEG (M_n = 5 kDa, 0.500 g, 0.1 mmol) and $AlMe_3$ (25 mg; 0.35 mmol) in toluene (10 mL). The mixture was stirred for 1 h, and then L- or D,L-lactide (1.00 g, 6.94 mmol) was added and the mixture was magnetically stirred at 70 °C for 48 h. Conversions were monitored by integration of the monomer vs. polymer methine resonances in the ^{1}H NMR spectrum of crude product (in $CDCl_3$). At complete monomer conversion, the mixture was poured into hexane (200 mL), and the precipitated polymer was recovered by filtration, washed with methanol, and dried at 40 °C in a vacuum oven. The copolymer was characterized by ^{1}H NMR spectroscopy.

^{1}H NMR ($CDCl_3$, 25 °C) δ = 1.54 (m, –$CHCH_3$–), 3.64 (s, –CH_2–), 5.15 (m, –$CHCH_3$–).

The molar percentage of lactide in each copolymer was evaluated by the relative intensity of signals at δ: 5.15 (–CH– of polylactide, A_{CH}) and 3.64 (–CH_2– of m-PEG, A_{CH2}).

Molecular weight was evaluated by ^{1}H NMR using the following equation:

$$Mn = (Mn_{PEG}\ (MW_{lactide})(2A_{CH}))/((A_{CH2})\ (MW_{ethyleneoxide})) + Mn_{PEG} \quad (1)$$

2.3. NMR Measurements

The ^{1}H-NMR spectra were recorded on a Bruker Avance 400 spectrometer (^{1}H, 400.00 MHz) at 25 °C using tetramethyl silane (TMS) as an internal reference (Aldrich).

Samples were prepared by introducing 20 mg of copolymer and 0.5 mL of $CDCl_3$ into an NMR-tube (5 mm outer diameter).

2.4. CMC Measurements

The critical micelle concentration (CMC) was determined using pyrene as a fluorescence probe. Samples for fluorescence spectroscopy were prepared by diluting the micelle solutions to 10 different concentrations (range 1.0×10^{-4} mol/L-1.0×10^{-7} mol/L). Each sample was then obtained by dropping a pyrene solution (5.0×10^{-6} mol/L in acetone) into an empty vial, adding one of the copolymer solutions previously prepared, and evaporating the acetone by gentle heating. The volume of the needed copolymer solution was calculated to have a final pyrene concentration in water of 6.0×10^{-7} mol/L, which is slightly below the pyrene saturation concentration at 22 °C. Fluorescence spectra were recorded using a Varian luminescence spectrometer at an excitation wavelength of 335 nm at 22 °C. The intensities of the bands I_1 at 372 nm and I_3 at 383 nm were evaluated and their ratios plotted vs. the copolymer concentration.

2.5. Preparation of BODIPY Loaded Micelles and Study of Release

A total of 800 µL of a 1 mg/mL solution of BODIPY in DCM and 1 mL of a solution containing the copolymer (solution prepared with 20 mg of polymer dissolved in 1 mL of DCM) were introduced in a dialysis membrane and dialyzed against PBS (pH 7.4) for 24 h.

In order to eliminate the residue of BODIPY, at the end of the dialysis, the sample was recovered from the membrane and centrifuged at 1000 rpm at 4 °C for 10 min. The supernatant was collected, and then 300 µL of a 2:1 DMSO:PBS solution was added to 300 µL of supernatant to determine the concentration of BODIPY loaded into the micelles.

The BODIPY loading was evaluated using the following equation:

$$\text{BODIPY loading } (\%) = \left[\frac{\text{mol of BODIPY loaded}}{\text{mol of micelles}}\right] \times 100 \quad (2)$$

To evaluate the amount of BODIPY released over time, at fixed times the solution containing the loaded micelles was centrifuged at 500 rpm at 5 °C for 5 min; the supernatant was removed while the precipitate was dissolved in 600 µL of 2:1 DMSO:PBS solution and analyzed by UV–vis spectroscopy at the λ = 548 nm of BODIPY maximum absorbance to determine the BODIPY concentration

2.6. Bacterial Strain and Growth Conditions

The photoinactivation assays were performed against the model pathogen *Staphylococcus aureus* ATCC6538P. *S. aureus* was grown overnight in tryptic soy broth (TSB) medium at 37 °C on an orbital shaker at 200 rpm. When necessary, a solid formulation (agar 15% *w*/*v*) was prepared.

2.7. Photoinactivation by Suspended Micelles

Upon overnight growth, *S. aureus* cultures were centrifuged (8000 rpm, 4 min), and the pellet was suspended in phosphate buffer saline (PBS, KH_2PO_4/K_2HPO_4 10 mM, pH 7.4) to reach a bacterial concentration of ~10^8 CFU/mL. BODIPY (1 or 0.1 µM) dissolved in DMSO or micelle encapsulated BODIPY (0.1 µM) was administered to cell suspensions. Samples were dark incubated for 10 min to favor the interaction between PSs and bacterial cells and then irradiated, at increasing times, under 520 nm light (2.4 mW/cm^2). At 1 h of irradiation, the final light dose was 8.7 J/cm^2, and at 6 h it was 52.1 J/cm^2. A panel of the following controls was kept under dark incubation: untreated cells, cells treated with DMSO (0.01% *v*/*v*) or with empty micelles, and cells treated with BODIPY (dissolved in DMSO or encapsulated). The effect of irradiation was also evaluated on untreated cells and cells treated with DMSO or empty micelles.

To determine the effect of dark incubation and irradiation on bacterial viability of control samples and PS-treated samples, cellular concentration was determined by viable

count technique. Each sample was collected and 10-fold serially diluted in PBS. A volume of 10 µL of each diluted and undiluted sample was plated on TSB agar plates. After overnight incubation at 37 °C, the cellular concentration was calculated and expressed as colony forming units per milliliter (CFU/mL). Photoinactivation experiments were performed at least in triplicate.

2.8. Photoinactivation Induced by Micelle-Coated Glass

A volume of 200 µL of PS-loaded micelles or free PS (0.8 µM) was sprayed on coverslip glasses. A sample without any coating was also included. Coated glasses were dried under airflow and positioned in 35 mm diameter petri dishes. Each dish was filled with 1.5 mL of bacterial suspension prepared by diluting 300-fold with an overnight *S. aureus* ATCC 6538P culture in M9 minimal medium added with 10 mM glucose and 0.2% *w/v* casamino acids. After overnight incubation at 37 °C, coverslip glasses were irradiated under light at 520 nm for 2 h in a humid chamber. Upon irradiation, adherent cells were stained for 30 min with 2 µM fluorochrome 4,4-difluoro-1,3,5,7-tetramethyl-8-(2-methoxyphenyl)-4-bora-3a,4a-diaza-s-indacene [26]. Then, the coverslips were transferred on microscope glass slides for confocal microscopy analysis. The images were acquired through a 63X objective lens and a 488 nm laser.

3. Results and Discussion

Most micelle coatings reported in the literature consist of physical adsorption of micelles to the surface [27–29]; in a few cases, the chemical coating is derived by the reaction of side or terminal groups of block copolymers forming micelles with groups on surfaces [30–32]. The general advantage of using micelles consists of their supramolecular typical structure that allows for the holding and releasing of active molecules.

In this study, the coating comprised micelles physically adsorbed on the surface and loaded with BODIPY. Controlled release of BODIPY in a relatively short range of time, during which the free molecule is activated by irradiation, allows bacteria decontamination of the surface, as reported in Scheme 1, avoiding the drawbacks connected to the $^1O_2$ diffusion through a polymer matrix and its partial deactivation.

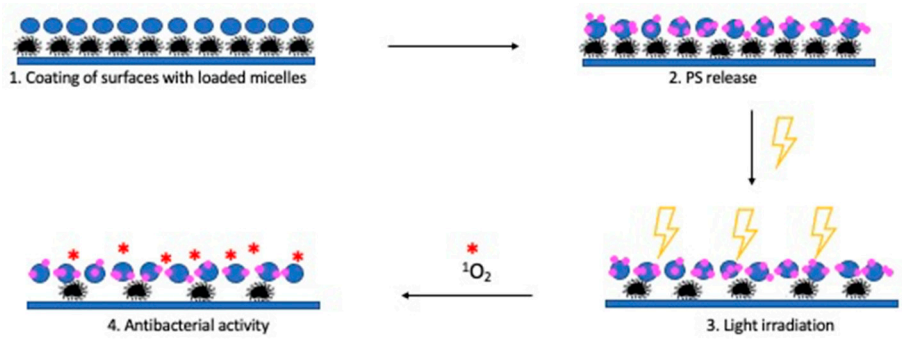

Scheme 1. Mechanism of action of the coating systems based on loaded micelles.

To this aim, we synthesized several linear and branched block copolymers of general structure AB_n (n = 1, 2, 4), where A is the poly(ethylene glycol)monomethylether (mPEG, 5 kDa) and B represents the poly(lactide) (PLA) blocks, either atactic poly D,L-lactide (PD,LLA) or stereoregular polyL-lactide (PLLA) (Figure 1). mPEG–$(PLA)_n$ linear and branched copolymers were synthesized following a procedure already reported by some of us [19] and with the rationale of obtaining a similar molecular weight for the hydrophobic and hydrophilic part of the copolymer to foster the formation of micelles by copolymer self-assembling in water. The idea of using micelles of mPEG–$(PLA)_n$ copolymers as surface releasing coatings is based on two consideration: the first one is about the degradability of copolymers, due to the presence of the polylactide blocks, that leads to a temporary coating; the second one is the presence of the mPEG block that preserves the surface from adsorption

of proteins and adhesion of cells after its decontamination and until the following process of surface disinfection. The linear and branched structures were synthesized, since we already noted that the copolymer structure can strongly influence chemical–physical properties as well as the biological behavior of supramolecular aggregates, such as micelles or vesicles or both when the copolymer is neutral and charged [19–21,33–43].

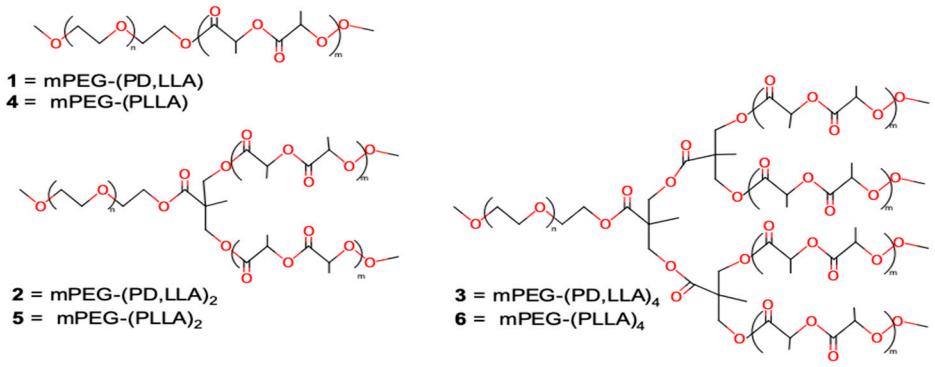

Figure 1. Copolymer structures. The numbers refer to the samples described in the relative entry of Table 1.

Table 1 shows data on microstructural features of the copolymers, the CMC of the corresponding micelles, and their ΔG formation. The last parameters are indicative of the thermodynamic stability of micelles and are fundamental for selecting copolymers that would maintain the supramolecular structure longer, allowing for the controlled release of PSs on the surface. The lower the CMC and ΔG values are, the higher the micelle stability is. It is well known that by controlling the crystallinity of the core it is possible to induce micelle stability. Data show that copolymers having the same general structure $A(B)_n$ possess lower CMC and ΔG when the polylactide chain is stereoregular (PLLA chains), which is noticeable when comparing CMC and ΔG values of entry 1 and 4, 2 and 5, and 3 and 6. Indeed, previous literature results showed that micelles formed with amorphous cores exhibited considerably higher CMCs than those with semicrystalline cores [44]. Among the stereoregular copolymers, mPEG–$(PLLA)_2$ and mPEG–$(PLLA)_4$ appeared the most appropriate for this study because of their lower CMC and ΔG. They are characterized by similar molecular weights but a different degree of branching and consequently different lengths of branches (17.4 and 13.4 monomer per arm for mPEG–$(PLLA)_2$ and mPEG–$(PLLA)_4$, respectively). It is worth noting that the two-arm branched, stereoregular copolymer mPEG–$(PLLA)_2$ shows the lowest CMC and ΔG, in accordance with what was previously found by some of us [20]. This experimental observation might be due to the presence of longer hydrophobic PLLA chains in the case of the two-arm branched copolymer compared to the four-arm branched ones. The longer PLLA arms may give rise to more inter-chain polymer entanglements, thus stabilizing the core and decreasing the CMC.

Table 1. Chemical structure, lactide content, and molecular weight (M_n) of copolymers. Critical micelle concentration (CMC) and ΔG formation of the corresponding micelles.

Entry	Copolymer [1]	LA unit/arm	M_n [2] (kDa)	CMC (M)	CMC (μg/mL)	ΔG [3] (kJ/mol)	BODIPY Loading [4] (%)
1	mPEG–(PD,LLA)	37.5	10.4	6.7×10^{-6}	70	−29.50	–
2	mPEG–$(PD,LLA)_2$	17.4	10.0	7.1×10^{-6}	71	−29.36	–
3	mPEG–$(PD,LLA)_4$	14.2	13.2	3.4×10^{-6}	39	−31.18	–
4	mPEG–(PLLA)	33.3	9.8	5.5×10^{-6}	54	−29.99	–
5	mPEG–$(PLLA)_2$	17.4	10.0	4.4×10^{-7}	4.4	−36.24	3.01
6	mPEG–$(PLLA)_4$	13.4	12.7	2.8×10^{-6}	36	−31.66	3.54

[1] mPEG molecular weight 5 kDa, [2] Evaluated by ^{1}H-NMR using Equation (1), [3] G = RTlnCMC, where CMC is expressed as mole fraction; T = 298 K, [4] Evaluated using Equation (2).

We loaded micelles obtained by self-assembling mPEG–$(PLLA)_2$ and mPEG–$(PLLA)_4$ in PBS (pH 7.4) with 2,6-diiodo-1,3,5,7-tetramethyl-8-(2,6-dichlorophenyl)-4,4′-difluoroboradiazaindacene (Figure 2), a PS belonging to the BODIPY family. This molecule showed a very high photodynamic activity against tumor cells, such us ovarian carcinoma cells (SKOV3), after irradiation with a green LED device [45], and thus it would be interesting to evaluate its antimicrobial activity against *Staphylococcus aureus* to assess whether neutral PSs, having an excellent antitumor efficacy, can also exert a strong antibacterial action. Our interest into antimicrobial activity against such bacteria derives from the fact that these pathogens are etiological agents of several nosocomial infections. Furthermore, the selection of strains resistant to a newer generation of antibiotics and the ability of *S. aureus* strains to form biofilm on inert surfaces and biological tissues makes their eradication more difficult [46].

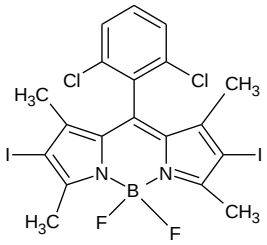

Figure 2. Structure of 2,6-diiodo-1,3,5,7-tetramethyl-8-(2,6-dichlorophenyl)-4,4′-difluoroboradiazaindacene (BODIPY) used as a photosensitizer (PS).

Table 1 shows data relative to the BODIPY loading for the two kind of copolymer forming micelles. The loading was quite similar for both micelles with a slightly higher amount of dye encapsulated in the more branched system. BODYPY release was studied in PBS solution at pH 7.4 and at room temperature (298 K) for 48 h, and it is reported in Figure 3. It is worth noting that both micellar systems could release the molecular dye in a controlled manner, with a massive but still contained release within the first half an hour, which was around 16% and 13% of the total content of BODIPY for mPEG–$(PLLA)_2$ and mPEG–$(PLLA)_4$ micelles, respectively. Interestingly, despite the lower amount of dye and higher stability, mPEG–$(PLLA)_2$ micelles were able to release almost 100% of BODIPY in the first 48 h, in contrast with the more branched ones that released only the 67% of total dye encapsulated in the same period of time. It is difficult to explain the different behavior of the two kinds of micelles in the release of BODIPY. One can suppose that the higher stability of mPEG–$(PLLA)_2$ micelles might be associated with the PLLA branch interactions in the core, which are stronger than those in the mPEG–$(PLLA)_4$. Thus, the strongest branch interactions may induce BODIPY molecules to accumulate preferentially in the outer part of the hydrophobic core, meaning close to the confined region between the hydrophobic region and the mPEG corona, during self-aggregation of mPEG–$(PLLA)_2$ copolymer.

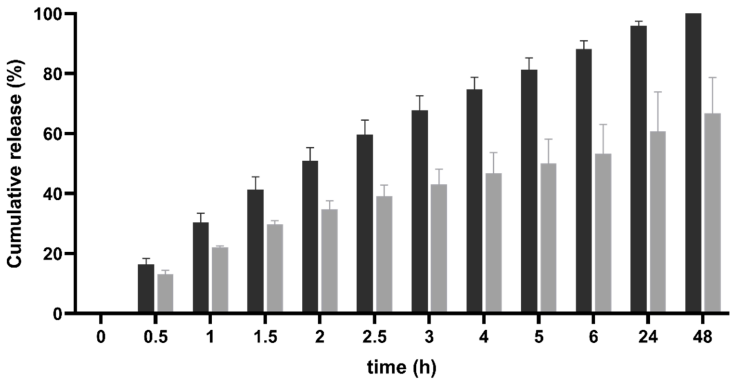

Figure 3. BODIPY release at pH 7.4 and 298 K from micelles made of mPEG–$(PLLA)_2$ (black) and mPEG–$(PLLA)_4$ (grey).

The different behavior in releasing BODIPY, as showed by the two systems, are both intriguing for a coating that requires a slow release of the antimicrobial PS. However, we decided to test the antimicrobial efficiency of the system based on the more stable micelles that release completely within 48 h.

To this aim, the efficiency of BODIPY in photoinactivation of the model strain *S. aureus* ATCC 6538P was tested, and data are reported in Figure 4. Under a low energy dose of light (8.7 J/cm^2) at 520 nm, BODIPY showed a dose-dependent killing effect. The lowest tested concentration (0.1 μM) caused a statistically significant reduction (p = 0.0361) of ~4 log unit, while the highest concentration (1 μM) caused the highest killing rate detectable in the chosen setup, namely ≤100 CFU/mL (p = 0.0023). All the included controls ruled out any intrinsic activity of BODIPY and of solvent used to solubilize PS (DMSO 0.01%). As expected, green light did not influence *S. aureus* viability. It is well known that neutral PSs belonging to several families, natural and synthetic, such as curcumin, hypericin, phthalocyanine, and fullerenes, are active against Gram-positive bacteria [47]. To the best of our knowledge, in this study, for the first time a neutral BODIPY was successfully tested as a PS against *S. aureus.* It is noteworthy to point out that the BODIPY was active at low micromolar concentration and was active only under irradiation. These features make the chosen BODIPY an interesting antimicrobial PS.

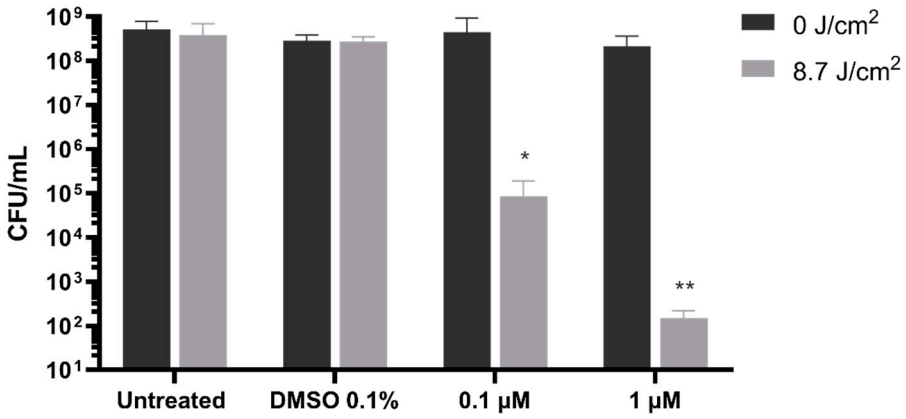

Figure 4. Photodynamic inactivation of *Staphylococcus aureus* by 0.1 and 1 μM of BODIPY dissolved in DMSO. Irradiation with light at 520 nm was performed for 1 h to reach a final dose of 8.7 J/cm^2. Untreated and DMSO (0.1% v/v)-treated samples were included as controls. Data of cell viability are expressed as CFU/mL ± standard deviations. Statistical analyses were performed by one-way ANOVA (* $p < 0.05$; ** $p < 0.01$).

To better appreciate the potential antimicrobial effect of micelle loading, the lowest tested concentration (0.1 μM) was preferred to the highest one (1 μM). To mimic a potential disinfection protocol, aPDI was performed at increasing irradiation times from 1 to 6 h. The dark incubation for long periods of time of PS dissolved in DMSO did not cause any alteration in bacterial viability, as shown in Figure 5. On the other hand, the irradiation of PS dissolved in DMSO showed a dose-dependent light killing rate; upon 3 h and longer time of irradiation (≥26.1 J/cm^2), the highest killing rate (limit of detection of the system) was reached. The antimicrobial effect of micelles was ruled out both under dark incubation and upon irradiation.

Interestingly, the encapsulation of PS in micelles did not impair the desired photoinactivation; a decrease of *S. aureus* viability was observed, even if to a lesser extent than what was elicited by PS dissolved in DMSO. The kinetics of photoinactivation induced by micelle-loaded PSs was like that observed with BODIPY in DMSO, reaching the highest rate (−5 log unit) after a 3 h and longer period of irradiation. A bacterial sample treated with empty micelles was also incubated in the dark or irradiated for 6 h, and no cellular concentration change was observed with respect to untreated cells (data not shown). In-

deed, it is important to rule out any bacterial agglutinating effect of micelles that could overestimate the antimicrobial effect.

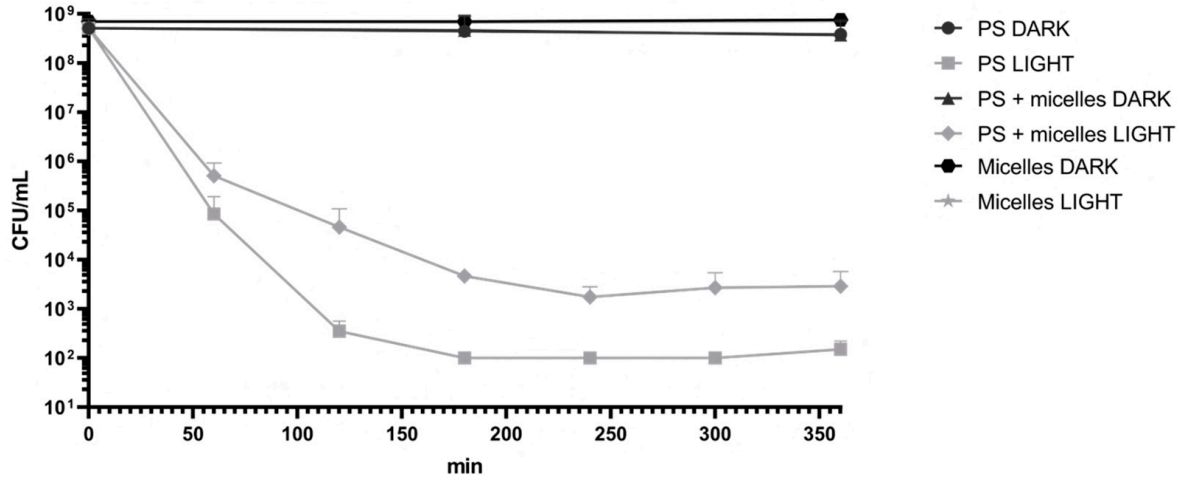

Figure 5. Photodynamic inactivation of *Staphylococcus aureus* with 0.1 μM BODIPY dissolved in DMSO or encapsulated in micelles. The irradiation with light at 520 nm was delivered up to 6 h, and the effect of micelle-encapsulated BODIPY and of BODIPY was checked every 60 min. Cell viability of control samples was checked upon 3 and 6 h of dark incubation or irradiation. Data are expressed as CFU/mL ± standard deviations.

The latter experiments showed that the delivery system of micelles worked very well; a decrease of 5 log unit from bacterial samples at a very high concentration (~10^9 CFU/mL) is an important microbiological goal. Furthermore, this delivery system represents a relevant alternative to DMSO as a carrier for BODIPY surface distribution, as DMSO has several drawbacks, such as environmental toxicity and difficult removal from surfaces.

To evaluate if the antimicrobial effect of the system could be observed upon coating, the following experiment was planned, as described in detail in Material and Methods. A coverslip glass was chosen as a surface to coat by spraying on it a water solution of micelles loaded with BODIPY and, thereafter, to inoculate with *S. aureus*. Upon overnight incubation, the irradiation (17.4 J/cm^2) by light at 520 nm caused clear alterations of cell integrity that were highlighted by confocal analysis. As can be appreciated in Figure 6A, the bacteria of the control sample showed the typical morphology of well-defined cocci and with a diameter of ~1–1.5 μm. In the enlarged image, it is possible to recognize couples of cells very close one to another, as expected, at the final step of the binary fission process. This is in accordance with viable and physiological undamaged bacteria. On the other hand, the distribution of the chosen fluorophore inside microorganisms inoculated on micelle coated surface was very different, as shown in Figure 6B. In this case, a diffuse signal of a fluorophore was detectable. It was not possible to identify the bacterial morphology, and, in addition, the dimensions of the photo-inactivated cells were smaller than those of the untreated ones. Furthermore, there was the appearance of clusters of cells not visible in the control sample. Induction of cell aggregation has already been observed in *S. aureus* strains [48] under adverse growth conditions, such as the presence of antibiotics in sub-toxic concentrations. The cluster formation thus represents a defensive strategy of bacteria to resist and is associated with the production of polysaccharides that favor cellular association and confer physical barrier properties to chemical agents. In the aggregate, there are dead and living cells, so that the polysaccharides and the presence of dead cells could explain the diffuse fluorescence we observed only in the case of coverslip glass coated with loaded micelles (Figure 6B).

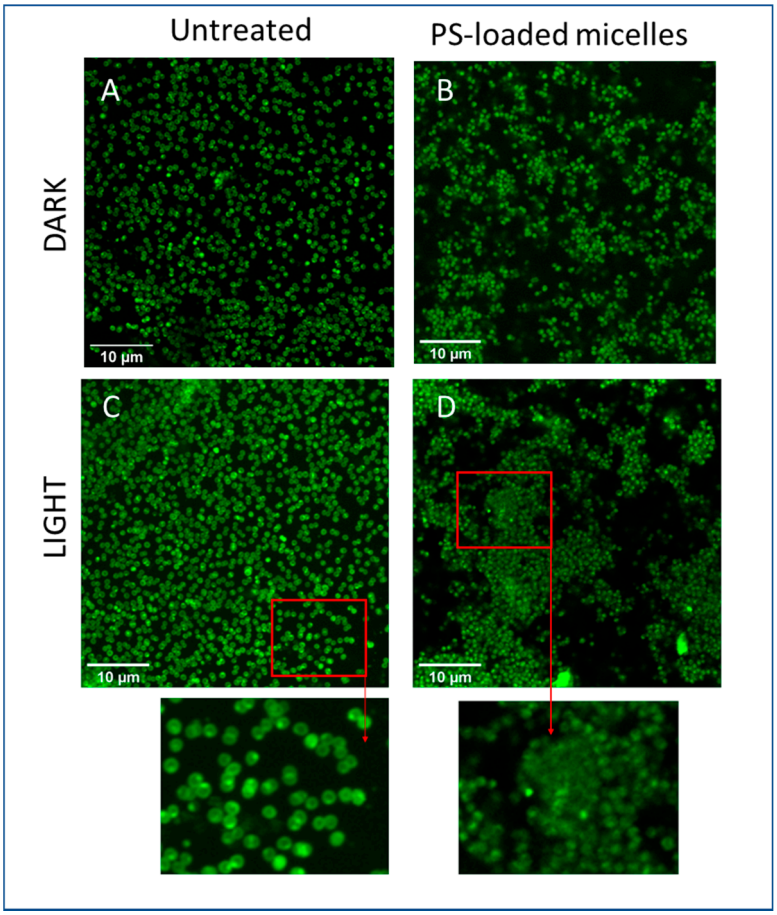

Figure 6. Photodynamic inactivation of *Staphylococcus aureus* grown on coverslip glasses. *S. aureus* cells were inoculated on coverslip glass (**A**,**C**) or on coverslip glass where a volume of 200 µL of PS-loaded micelle (0.8 µM) solutions was sprayed on (**B**,**D**). Upon overnight growth, cells were irradiated under light at 520 nm for 2 h (**C**,**D**) or dark incubated (**A**,**B**). The fluorochrome was added 30 m before confocal analysis. The images were acquired through a 63X objective lens and a 488 nm laser.

Taken together, these observations suggest that the coated surface changed greatly the appearance and most likely compromised the physiological status of the microbial population.

The combination of micelles and PSs seems very promising in the antimicrobial field and suggests further improvements. Since polymers with intrinsic photosensitizing activity have been investigated [49,50], a novel potential antimicrobial technique could rely on synergistic activity of photoactivable micellar components combined with PSs. This approach could take advantage of the antimicrobial activity of both involved parts, the container and the content.

4. Conclusions

In this study, we report a strategy to decontaminate surfaces from *S. aureus*, one of the more difficult human pathogens to eradicate, by a coating made of micelles loaded with the neutral BODIPY 2,6-diiodo-1,3,5,7-tetramethyl-8-(2,6-dichlorophenyl)-4,4′-difluoroboradiazaindacene. Micelles formed from mPEG–$(PLLA)_n$ with mPEG 5kDa and n = 2 or 4 were found to be the most thermodynamically stable among those obtained by self-assembling several copolymers based on mPEG and PLA branches, the latter both atactic and stereoregular. The higher stability of micelles obtained from the stereoregular branched copolymers might be ascribed to the stronger hydrophobic interaction among the PLLA arms with respect to the corresponding atactic copolymer, and for the presence of more than one PLLA chain per mPEG block. Release of BODIPY from micelles obtained

by self-assembling the stereoregular branched copolymers in solution showed a very different behavior depending on the copolymer structure. Interestingly, the most stable supramolecular system, based on mPEG–$(PLLA)_2$, was able to release faster, probably for a different localization of the dye within the micelles. PSs are likely placed in the outer part of the hydrophobic core and in proximity to the hydrophilic corona. The faster releasing system was the one tested in the antimicrobial activity, and two significant results emerged from experimental data. For the first time it was demonstrated that a neutral BODIPY, after irradiation, is active against *S. aureus* even at micromolar concentrations, and that the system releasing such a BODIPY induces an important decrease of 5 log unit in the presence of a high concentration (~10^9 CFU/mL) of bacteria.

Overall, the supramolecular BODIPY releasing system proposed in this paper as a coating for surface decontamination allows for the overcoming of several complications deriving from the use of photodynamic active coating containing PSs, meaning ROS diffusion through the polymer matrix responsible for their partial deactivation or oxygen matrix permeability required to produce $^1O_2$.

More in general, such a system is highly versatile, since in principle it is possible to modulate PS release by properly choosing the structure of copolymer forming micelles and the nature of PSs.

Author Contributions: E.C. and V.T.O. equally contributed. M.C.M. and E.M. are students in "Life Science and Biotechnology"; C.S. is a student in "Chemistry and Environmental Chemistry". Conceptualization, E.C., V.T.O., L.I., D.P. and G.V.; Investigation, M.C.M. and E.M.; Methodology, E.C., V.T.O. and L.I.; Supervision, E.C., V.T.O. and L.I.; Validation, M.C.M. and E.M.; Visualization, C.S., D.P. and G.V.; Writing—original draft, L.I.; Writing—review and editing, L.I. All authors have read and agreed to the published version of the manuscript.

Funding: This research received no external funding.

Institutional Review Board Statement: Not applicable.

Informed Consent Statement: Not applicable.

Data Availability Statement: Data is contained within the article.

Acknowledgments: D.P. acknowledges funding from the "Fondo di Ateneo per la Ricerca di Base (FARB 2017)". L.I. acknowledges funding from the "Fondo di Ateneo per la Ricerca (FAR 2018)".

Conflicts of Interest: The authors declare no conflict of interest.

References

1. Russel, A.D. Bacterial resistance to disinfectant. *J. Infect. Prev.* **2002**, *3*, 22–24. [CrossRef]
2. Campoccia, D.; Montanaro, L.; Arciola, C.R. A review of the biomaterial technologies for infection-resistant surfaces. *Biomaterials* **2013**, *34*, 8533–8554. [CrossRef] [PubMed]
3. Tamanna, T.; Bulitta, J.B.; Landersdorfer, C.B.; Cashin, V.; Yu, A. Stability and controlled antibiotic release from thin films embedded with antibiotic loaded mesoporous silica nanoparticles. *RSC Adv.* **2015**, *5*, 107839–107846. [CrossRef]
4. Banfi, S.; Caruso, E.; Orlandi, V.T.; Barbieri, P.; Cavallari, S.; Viganò, P.; Clerici, P.; Chiodaroli, L. Antibacterial activity of leaf extracts from Combretum micranthum and Guiera senegalensis (Combretaceae). *Res. J. Microbiol.* **2014**, *9*, 66–81. [CrossRef]
5. Takahashi, H.; Caputo, G.A.; Vemparala, S.; Kuroda, K. Synthetic Random Copolymers as a Molecular Platform to Mimic Host-Defense Antimicrobial Peptides. *Bioconjug. Chem.* **2017**, *28*, 1340–1350. [CrossRef]
6. Caruso, E.; Malacarne, M.C.; Banfi, S.; Gariboldi, M.B.; Orlandi, V.T. Cationic diarylporphyrins: In vitro versatile anticancer and antibacterial photosensitizers. *J. Photochem. Photobiol. B* **2019**, *197*, 111548. [CrossRef]
7. Cieplik, F.; Deng, D.; Crielaard, W.; Buchalla, W.; Hellwig, E.; Al-Ahmad, A.; Maisch, T. Antimicrobial photodynamic therapy—what we know and what we don't. *Crit. Rev. Microbiol.* **2018**, *44*, 571–589. [CrossRef] [PubMed]
8. Hamblin, M.R.; Abrahamse, H. Can light-based approaches overcome antimicrobial resistance? *Drug Dev. Res.* **2018**, *80*, 48–67. [CrossRef]
9. Gerola, A.P.; Costa, P.F.A.; de Morais, F.A.P.; Tsubone, T.M.; Caleare, A.O.; Nakamura, C.V.; Brunaldi, K.; Caetano, W.; Kimura, E.; Hioka, N. Liposome and polymeric micelle-based delivery systems for chlorophylls: Photodamage effects on Staphylococcus aureus. *Colloids Surfaces B Biointerfaces* **2019**, *177*, 487–495. [CrossRef]
10. Gao, Y.; Wang, J.; Hu, D.; Deng, Y.; Chen, T.; Jin, Q.; Ji, J. Bacteria-Targeted Supramolecular Photosensitizer Delivery Vehicles for Photodynamic Ablation Against Biofilms. *Macromol. Rapid Commun.* **2018**, *40*, 1800763. [CrossRef] [PubMed]

11. McCoy, P.C.; O'Neil, E.J.; Cowley, J.F.; Carson, L.; De Baroid, A.T.; Gdowski, G.T.; Gorma, S.P.; Jones, D.S. Photodynamic Antimicrobial Polymers for Infection. *PLoS ONE* **2014**, *9*, e108500. [CrossRef]
12. Qin, Y.; Chen, L.L.; Pu, W.; Liu, P.; Liu, S.X.; Li, Y.; Liu, X.L.; Lu, Z.X.; Zheng, L.Y.; Cao, Q.E. A hydrogel directly assembled from a copper metal-organic polyhedron for antimicrobial application. *Chem. Commun.* **2019**, *55*, 2206–2209. [CrossRef]
13. Henke, P.; Kirakci, K.; Kubat, P.; Fraiberk, M.; Forstovà, J.; Mosinger, J. Antibacterial, antiviral, and oxygen-sensing nanoparticles prepared from electrospun materials. *ACS Appl. Mater. Interfaces* **2016**, *8*, 25127–25136. [CrossRef] [PubMed]
14. Zhang, F.; Zhang, C.L.; Peng, H.Y.; Cong, H.P.; Qian, H.S. Near-infrared photocatalytic upconversion nanoparticles/TiO_2 nanofibers assembled in large scale by electrospinning. *Part. Part. Syst. Charact.* **2016**, *33*, 248–253. [CrossRef]
15. Dolansky, J.; Henke, P.; Malà, Z.; Zàrskà, L.; Kubàt, P.; Mosinger, J. Antibacterial nitric-oxide- and singlet oxygen-releasing polystyrene nanoparticles responsive to light and temperature triggers. *Nanoscale* **2018**, *10*, 2639–2648. [CrossRef] [PubMed]
16. Thomas, D.D.; Liu, X.Q.; Kantrow, S.P.; Lancaster, J.R. The biological lifetime of nitric oxide: Implications for the perivascular dynamics of NO and O_2. *Proc. Natl. Acad. Sci. USA* **2001**, *98*, 355–360. [CrossRef] [PubMed]
17. Bregnhoj, M.; Westberg, M.; Jensen, F.; Ogilby, P.R. Solvent-dependent singlet oxygen lifetimes: Temperature effects implicate tunneling and charge-transfer interactions. *Phys. Chem. Chem. Phys.* **2016**, *18*, 22946–22961. [CrossRef]
18. Felgenträger, A.; Maisch, T.; Späth, A.; Schröder, J.A.; Bäumler, W. Singlet oxygen generation in porphyrin-doped polymeric surface coating enables antimicrobial effects on *Staphylococcus aureus*. *Phys. Chem. Chem. Phys.* **2014**, *16*, 20598–20607. [CrossRef]
19. Izzo, L.; Pappalardo, D. "Tree-Shaped" Copolymers Based on Poly(ethylene glycol) and Atactic or Isotactic Polylactides: Synthesis and Characterization. *Macromol. Chem. Phys.* **2010**, *211*, 2171–2178. [CrossRef]
20. Garofalo, C.; Capuano, G.; Sottile, R.; Tallerico, R.; Adami, R.; Reverchon, E.; Carbone, E.; Izzo, L.; Pappalardo, D. Different Insight into Amphiphilic PEG-PLA Copolymers: Influence of Macromolecular Architecture on the Micelle Formation and Cellular Uptake. *Biomacromolecules* **2014**, *15*, 403–415. [CrossRef]
21. Adami, R.; Liparoti, S.; Izzo, L.; Pappalardo, D.; Reverchon, E. PLA-PEG copolymers micronization by Supercritical Assisted Atomization. *J. Supercrit. Fluids* **2012**, *72*, 15–21. [CrossRef]
22. Caruso, E.; Banfi, S.; Barbieri, P.; Leva, B.; Orlandi, V.T. Synthesis and antibacterial activity of novel cationic BODIPY photosensitizers. *J. Photochem. Photobiol. B* **2012**, *114*, 44–51. [CrossRef] [PubMed]
23. Orlandi, V.T.; Rybtke, M.; Caruso, E.; Banfi, S.; Tolker-Nielsen, T.; Barbieri, P. Antimicrobial and anti-biofilm effect of a novel BODIPY photosensitizer against Pseudomonas aeruginosa PAO1. *Biofuling* **2014**, *30*, 883–891. [CrossRef] [PubMed]
24. Caruso, E.; Ferrara, S.; Ferruti, P.; Manfredi, A.; Ranucci, E.; Orlandi, V.T. Enhanced photoinduced antibacterial activity of a BODIPY photosensitizer in the presence of polyamidoamines. *Lasers Med. Sci.* **2018**, *33*, 1401–1407. [CrossRef] [PubMed]
25. Banfi, S.; Nasini, G.; Zaza, S.; Caruso, E. Synthesis and Photo-Physical properties of a series of BODIPY dyes. *Tetrahedron* **2013**, *69*, 4845–4856. [CrossRef]
26. Orlandi, V.T.; Martegani, E.; Bolognese, F.; Trivellin, N.; Paldrychova, M.; Matatkova, O.; Baj, A.; Caruso, E. Photodynamic therapy by diaryl-porphyrins to control Candida albicans growth. *Cosmetics* **2020**, *7*, 31. [CrossRef]
27. Meiners, J.C.; Quintel-Ritzi, A.; Mlynek, J.; Elbs, H.; Kraisch, G. Adsorption of block-copolymer micelles from a selective solvent. *Macromolecules* **1997**, *30*, 4945–4951. [CrossRef]
28. Farinha, J.P.S.; D'Oliveira, J.M.R.; Martinoho, J.M.; Xu, R.; Winnik, M.A. Structure in tethered chains: Polymeric micelles and chains anchored on polystyrene latex spheres. *Langmuir* **1998**, *14*, 2291–2296. [CrossRef]
29. Li, Y.; Pi, Q.; You, H.; Li, J.; Wang, P.; Yang, X.; Wu, Y. A smart multi-functional coating based on anti-pathogen micelles tethered with copper nanoparticles via a biosynthesis method using L-vitamin C. *RSC Adv.* **2018**, *8*, 18272–18283. [CrossRef]
30. Webber, S.E. Polymer micelles: An example of self-assembling polymers. *J. Phys. Chem. B* **1998**, *102*, 2618–2626. [CrossRef]
31. Karymov, M.A.; Prochazka, K.; Mendenhall, J.M.; Martin, T.J.; Munk, P.; Webber, S.E. Chemical Attachment of Polystyrene-*block*-poly(methacrylic acid) Micelles on a Silicon Nitride Surface. *Langmuir* **1996**, *12*, 4748–4753. [CrossRef]
32. Emoto, K.; Nagasaki, Y.; Kataoka, K. Coating of Surfaces with Stabilized Reactive Micelles from Poly(ethylene glycol)-Poly(DL-lactic acid) Block Copolymer. *Langmuir* **1999**, *15*, 5212–5218. [CrossRef]
33. Izzo, L.; Gorrasi, G.; Sorrentino, A.; Tagliabue, A.; Mella, M. Controlling Drug Release of Anti-inflammatory Molecules Through a pH-Sensitive, Bactericidal Polymer Matrix: Towards a Synergic and Combined Therapy. *Lect. Notes Bioeng.* **2019**, 151–163. [CrossRef]
34. Mella, M.; Tagliabue, A.; Mollica, L.; Izzo, L. Monte Carlo study on the effect on macroion charge distribution on the ionization and adsorption of weak polyelectrolytes and concurrent counterion release. *J. Colloids Interface Sci.* **2020**, *560*, 667–680. [CrossRef]
35. Tagliabue, A.; Izzo, L.; Mella, M. Impact of charge correlation, chain rigidity, and chemical specific interactions on the behaviour of weak polyelectrolytes in solution. *J. Phys. Chem. B* **2019**, *123*, 8872–8888. [CrossRef] [PubMed]
36. Izzo, L.; Matrella, S.; Mella, M.; Benvenuto, G.; Vigliotta, G. *Escherichia coli* as a Model for the Description of the Antimicrobial Mechanism of a Cationic Polymer Surface: Cellular Target and Bacterial Contrast Response. *ACS Appl. Mat. Interfaces* **2019**, *11*, 15332–15343. [CrossRef]
37. Barrella, M.C.; Di Capua, A.; Adami, R.; Reverchon, E.; Mella, M.; Izzo, L. Impact of intermolecular drug-copolymer interactions on size and drug release kinetics from pH-responsive polymersomes. *Supramol. Chem.* **2017**, *29*, 796–807. [CrossRef]
38. Villani, S.; Adami, A.; Reverchon, E.; Ferretti, A.M.; Ponti, A.; Lepretti, M.; Caputo, I.; Izzo, L. pH-sensitive polymersomes: Controlling swelling via copolymer structure and chemical composition. *J. Drug Target.* **2017**, *25*, 899–909. [CrossRef]

39. Tagliabue, A.; Izzo, L.; Mella, M. Out of equilibrium self-assembly of Janus nanoparticles: Steering it from disordered amorphous to 2D patterned aggregates. *Langmuir* **2016**, *32*, 12934–12946. [CrossRef] [PubMed]
40. Matrella, S.; Vitiello, C.; Mella, M.; Vigliotta, G.; Izzo, L. The Role of Charge Density and Hydrophobicity on the Biocidal Properties of Self-Protonable Polymeric Materials. *Macromol. Biosci.* **2015**, *15*, 927–940. [CrossRef]
41. Mella, M.; Mollica, L.; Izzo, L. Influence of charged intramolecular hydrogen bonds in weak polyelectrolytes: A Monte Carlo study of flexible and extendible polymeric chains in solution and near charged spheres. *J. Polymer Sci. Part B Polymer Phys.* **2015**, *53*, 650–663. [CrossRef]
42. Izzo, L.; Gorrasi, G. Effect of molecular architecture on physical properties of tree-shaped and star-shaped poly(methylmethacrylate)-based copolymers. *J. Macromol. Sci. B* **2014**, *53*, 474–485. [CrossRef]
43. Vigliotta, G.; Mella, M.; Rega, D.; Izzo, L. Modulating antimicrobial activity by synthesis: Dendritic copolymers based on nonquaternized 2-(dimethylamino)ethyl methacrylate by Cu-mediated ATRP. *Biomacromolecules* **2012**, *13*, 833–841. [CrossRef]
44. Glavas, L.; Olsén, P.; Odelius, K.; Albertsson, A.-C. Achieving Micelle Control through Core Crystallinity. *Biomacromolecules* **2013**, *14*, 4150–4156. [CrossRef] [PubMed]
45. Caruso, E.; Gariboldi, M.B.; Sangion, A.; Gramatica, P.; Banfi, S. Synthesis, photodynamic activity, and quantitative structure-activity relationship modelling of a series of BODIPYs. *J. Photochem. Photobiol. B* **2017**, *167*, 269–281. [CrossRef]
46. Álvarez, A.; Fernández, L.; Gutiérrez, D.; Iglesias, B.; Rodríguez, A.; García, P. Methicillin-Resistant Staphylococcus aureus in Hospitals: Latest Trends and Treatments Based on Bacteriophages. *J. Clin. Microbiol.* **2019**, *57*, e01006-19. [CrossRef]
47. Ghorbani, J.; Rahban, B.; Aghamiri, S.; Teymouri, A.; Bahador, A. Photosensitizers in antibacterial photodynamic therapy: An overview. *Laser Ther.* **2018**, *27*, 293–302. [CrossRef]
48. Haaber, J.; Thorup Cohn, M.; Frees, D.; Andersen, T.J.; Ingmer, H. Planktonic Aggregates of *Staphylococcus aureus* Protect against Common Antibiotics. *PLoS ONE* **2012**, *7*, e41075. [CrossRef]
49. Zhao, Q.; Li, J.; Zhang, X.; Li, Z.; Tang, Y. Cationic Oligo(thiophene ethynylene) with Broad-Spectrum and High Antibacterial Efficiency under White Light and Specific Biocidal Activity against S. aureus in Dark. *ACS Appl. Mater. Interfaces* **2016**, *8*, 1019–1024. [CrossRef] [PubMed]
50. Zhou, Z.; Ergene, C.; Lee, J.Y.; Shirley, D.J.; Carone, B.R.; Caputo, G.A.; Palermo, E.F. Sequence and Dispersity Are Determinants of Photodynamic Antibacterial Activity Exerted by Peptidomimetic Oligo(thiophene)s. *ACS Appl. Mater. Interfaces* **2019**, *11*, 1896–1906. [CrossRef] [PubMed]